Electronic Supplementary Information

1. Instrumentation

Solid-state NMR was measured at room temperature through direct excitation (DE) or cross-polarization (CP) of the ^{51}V nuclei using a 4 mm Bruker double resonance iProbe at a 9.4 T magnet. The ^{51}V 90° DE pulse length was calibrated using V_2O_5. To capture the wide sideband pattern, variable offset stepwise acquisition was used. The spectral widths of each individual spectrum varied between 1200 and 2400 ppm; the offset was changed in steps of 700-1800 ppm. To identify isotropic chemical shifts all samples were measured at two or more different MAS frequencies. For the CP, a 2 ms ramp (50 to 100%) on the ^{1}H channel was used during the CP contact time. For heteronuclear decoupling during acquisition, SPINAL64 was employed with a 100 kHz nutation frequency (^{1}H). ^{1}H-^{51}V FSLG HETCOR data using SPINAL64 heteronculear decoupling and a CP contact time of 2 ms were recorded with 120 co-added transients for each of the 92 t_1 FIDs. The interscan delay of 2 s results in an overall experimental time of ca. 6 h.

Solution-phase NMR spectra were recorded using JEOL JNM-LA400. ^{51}V NMR spectra were measured at 105.15 MHz. Chemical shifts were referenced to $VOCl_3$ (δ = 0 ppm) for ^{51}V NMR.

Cold-spray ionization mass spectrometry (CSI-MS) was recorded on a JEOL JMS-T100CS. The samples were dissolved in DMF and the cold-spray temperature was -10°C.

Single-crystal X-ray diffraction (sc-XRD) was measured on a Bruker APEX-II CCD Single-crystal X-ray diffractometer equipped with a graphite monochromator using Mo Kα radiation (wavelength λ(Mo Kα) = 0.71073 Å)

Thermogravimetric analysis: (TGA) was carried out on a NETZSCH TG 209F1 analyzer at a heating rate of 10.0 K min-1 in a range between 30 and 600 °C under O2/N2 in an Al crucible.

Microscope/Camera: Photos of the single-crystals are taken by a Bresser Microscope - 5803100 - Researcher ICD LED 20x-80x equipped with a Bresser Full HD Microscope Telescope Camera USB 2.0 with Built-in UV/IR Filter.

Attenuated total reflectance-Fourier-transformed infrared spectroscopy (ATR-FT-IR) were performed using a Bruker Alpha II equipped with an ATR Platinum Diamond unit. The data were recorded with 24 scans at a resolution of 4 cm^{-1}. A background correction was used for all spectra from the OPUS 8.1 program.

Energy-dispersive X-ray spectroscopy (EDX) was performed on a Zeiss Leo-1530 scanning electron microscope (equipped with an Oxford Instruments X-maxN EDX detector (operated at 10 kV).

Hirshfeld Surface Analysis was performed by CrystalExplorer Software Version 21. [S1]

2. Synthetic section

General remarks: All chemicals were purchased from Sigma Aldrich, ABCR or Carl Roth and were of reagent grade. The chemicals were used without further purification unless stated otherwise. $(n\mathrm{Bu_4N})_4[\mathrm{V_4O_{12}}]$ = **{$\mathbf{V_4}$}** was prepared according to reference S2. $(n\mathrm{Bu_4N})_5\{\mathrm{V_{12}O_{32}(NO_3)}\}$ and $(n\mathrm{Bu_4N})_5\{\mathrm{V_{12}O_{32}(Br)}\}$ were prepared according to reference S3 and S4 and changing the synthesis slightly by using Tetrabutylammonium salt instead of Tetraethalammonium. Furthermore adding of Diethyl ether is crucial to precipitate the product as oil.

Synthesis of $\mathrm{La(DMSO)_8(C_8H_{22}N_4)\{(V_{12}O_{32}(Br)\}}$ (1):

$(n\mathrm{Bu_4N})_4[\mathrm{V_4O_{12}}]$ (200 mg, 0.139 mmol, 1.00 eq.), $\mathrm{LaBr_3}$ (52.6 mg, 0.139 mmol, 1.00 eq.) and Cyclen (24.0 mg, 0.139 mmol, 1.00 eq.) were dissolved in DMSO and stirred at 80 °C. The yellowish solution was cooled to rt after 4 hours and acidified with ca. five drops of 48 % HBr solution. The solution became over white cloudy, red to an orange solution and was stored in a dark ambient for one to five days. Dark orange red cubic crystals were filtrated and washed with DMSO and Ether three times. Yield: 20.1 mg, 0.00939 mmol, 20.3 % based on V).

MW = 2141.45 g/mol

Elemental analysis (EDX): metal ratio (at.-%): La:V: obs.: 1.0:11.43 (obsd); 1.0:12.0 (calcd)

Characteristic IR bands (in $\mathrm{cm^{-1}}$): 3291 (N-H stretching, secondary amine); 2999 (C-H stretching, alkane); 2913 (C-H stretching, alkane); 1587 (N-H bending, amine); 1399 (-); 1316 (C-N stretching aromatic, amine); 1143 (C-N stretching, amine); 1124 (C-N stretching, amine); 974 (V=O, terminals Oxygen); 953 (V=O, terminals Oxygen); 848 (-); 752 (V-O-V, symmetric); 705 (N-H wagging, sek. amine); 607 ($\mathrm{V_3}$-$\mathrm{O_{\mu 3}}$, asymmetric); 506 (-)

*Figure S 1: Microscope Picture of compound **1**.*

Synthesis $Ba(DMSO)_8(C_8H_{23}N_4)\{(V_{12}O_{32}(Br)\}$ (2):

(nBu$_4$N)$_4$[V$_4$O$_{12}$] (200 mg, 0.139 mmol, 1.00 eq.), $BaBr_2 \cdot 2\ H_2O$ (41.3 mg, 0.139 mmol, 1.00 eq.) and Cyclen (24.0 mg, 0.139 mmol, 1.00 eq.) were dissolved in DMSO and stirred at 80 °C. The yellowish solution was cooled to rt after 4 hours and acidified with ca. six drops of 48 % HBr solution. The solution became over white cloudy, red to an orange solution and was stored in a dark ambient for one to five days. Dark orange red cubic crystals were filtrated and washed with DMSO and Ether three times. Yield: 2.60 mg, 1.21 µmol, 0.874 % based on V).

MW = 2140.88 g/mol

Characteristic IR bands (in cm^{-1}): 3288 (N-H stretching, secondary amine); 3002 (C-H stretching, alkane); 2914 (C-H stretching, alkane); 1547 (N-H bending, amine); 1434 (-); 1412 (-); 1400 (-); 1351 (-); 1311 (C-N stretching aromatic, amine); 1023 (S=O, DMSO); 984 (V=O, terminals Oxygen); 953 (V=O, terminals Oxygen); 853 (-); 787 (-); 749 (V-O-V, symmetric); 704 (N- H wagging, amine); 630 (V_3-$O_{\mu3}$, asymmetric); 538 (-); 508 (-); 405 (-)

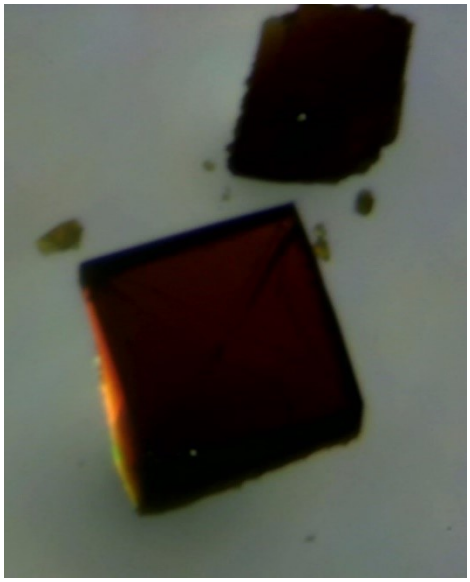

*Figure S 2: Microscope picture of compound **2**.*

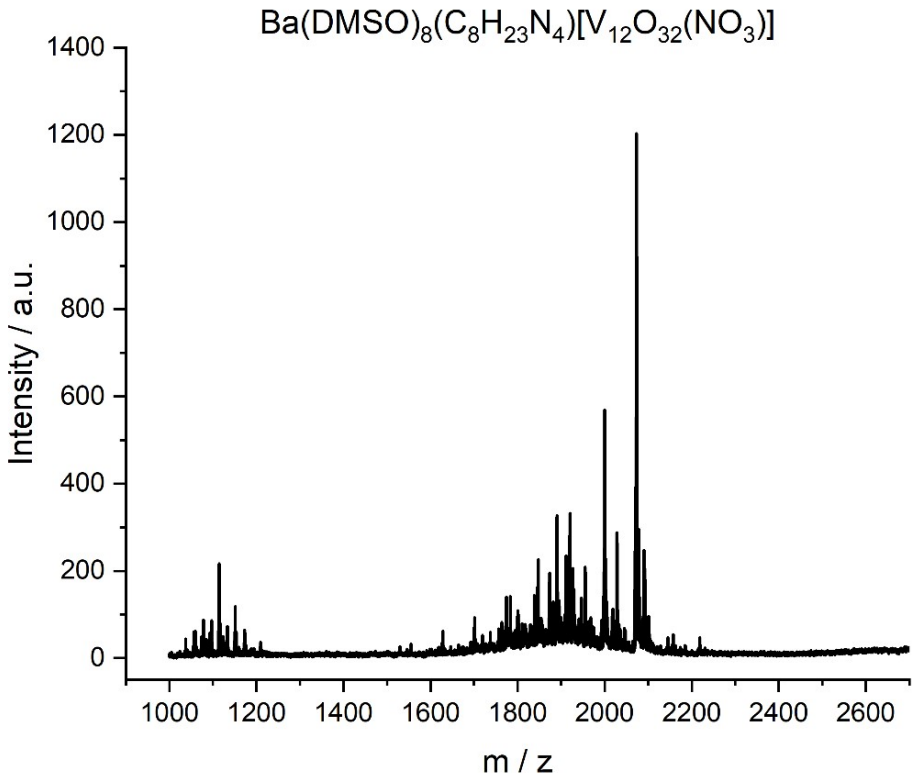

*Figure S 3: CSI mass spectrum of compound **2***

*Table S 1: CSI Mass spectrometric peak assignments for compound **2***

m / z (observed)	m / z (calculated)	fragment
2000.32	2000.41	$[Ba_2(DMF)_5(C_8H_{22}N_4)V_{12}O_{32}(NO_3)]^{1+}$
2073.35	2073.46	$[Ba_2(DMF)_6(C_8H_{22}N_4)V_{12}O_{32}(NO_3)]^{1+}$

Synthesis of $La(DMSO)_8(C_8H_{22}N_4)\{(V_{12}O_{32}(Cl)\}$ (3):

$(n Bu_4N)_4[V_4O_{12}]$ (200 mg, 0.139 mmol, 1.00 eq.), $LaCl_3 \cdot 7H_2O$ (34.1 mg, 0.0918 mmol, 0.66 eq.) and Cyclen (24.0 mg, 0.139 mmol, 1 eq.) were dissolved in DMSO and stirred at 80 °C. The yellowish solution was cooled to rt after 4 hours and acidified with 4-6 drops of 6 M HCl until the solution. The solution became over white cloudy, red to an orange solution. Diffusion crystallisation with Acetone yielded single-crystals suitable for sc-XRD. The substance could be synthesized in only a very small scale, which could not be further characterized. Yield: 1.70 mg, 0.811 µmol (8 DMSO were used as weight), 0.583 % based on V).

MW = 2097.00 g/mol

Characteristic IR bands (in cm^{-1}):

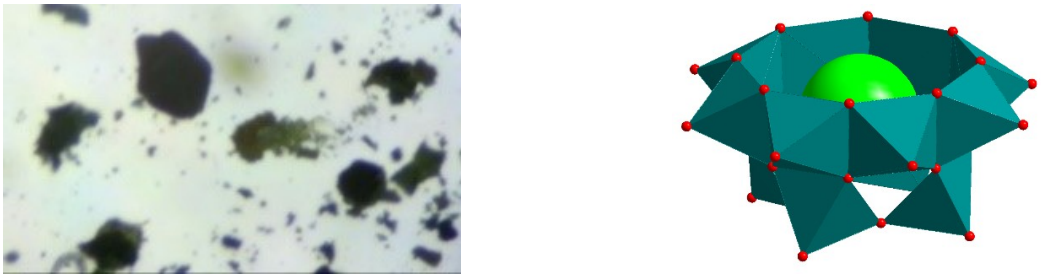

*Figure S 4: Microscope picture and sc-XRD presentation of compound **3**.*

Synthesis of protonated cyclen salts:

The protonation was done by acidification of cyclen with an excess amount of the acid with the specific anion. HNO_3, HCl and HBr were used to synthesize $H_4Cyclen(NO_3/Cl/Br)_4$. The synthesis is a modification of a literature-known route[S5]:

General Protonation Route:
48.0 mg (0.279 mmol) cyclen is dissolved in 5 mL D.I. water under stirring. The respective concentrated acid is added in excess and the solution is stirred for 30 min. A white precipitate is formed which is filtered off, washed and dried under vacuum.

$H_4Cyclen(NO_3)_4$:

MW: 424.32 g/mol

Yield: 94.3 mg (0.222 mmol, 79.7 %)

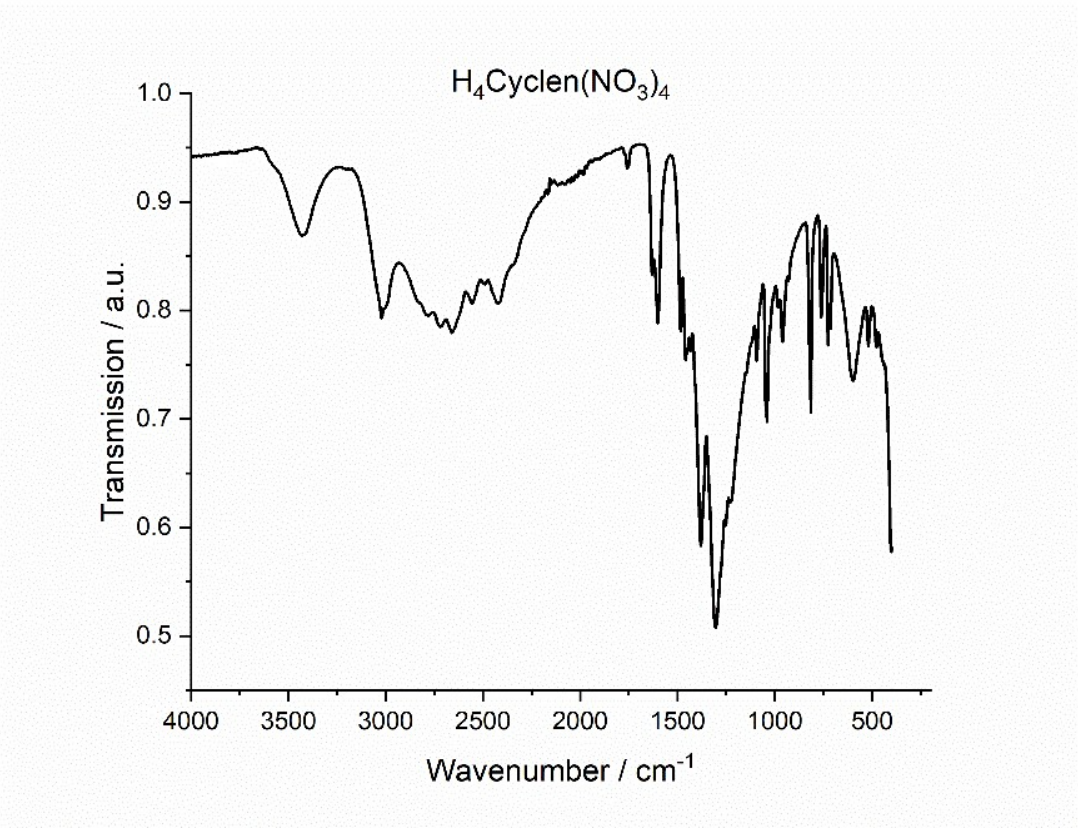

Figure S 5: FT-IR spectra of H_4cyclen$(NO_3)_4$.

Characteristic IR bands (in cm^{-1}):

3432 (water); 3024 (N-H Stretch, secondary Amine); 3004 (N-H stretching, amine salt); 2836 (N-H stretching amine salt); 2788 (N-H stretching amine salt); 2719 (secondary NH_2^+ overtone); 2661 (secondary NH_2^+ overtone); 2555 (secondary NH_2^+ overtone); 2493 (secondary NH_2^+ overtone); 2421 (secondary NH_2^+ overtone); 1760 (-) ; 1632 (water); 1602 (N-H bending, amine); 1483 (-); 1458 (-); 1431 (-); 1382; 1306 (C-N stretching aromatic, amine); 1254 (-); 1227 (-); 1093 (C-N stretching, amine); 1038 (C-N stretching, amine); 983 (-); 959 (-); 816 (-); 761 (-); 728 (-); 713 (-); 597 (-); 518 (-); 481 (-)

H_4Cyclen$(Cl)_4$:

MW: 318.11 g/mol

Yield: 35.4 mg (0.111 mmol, 39.9 %)

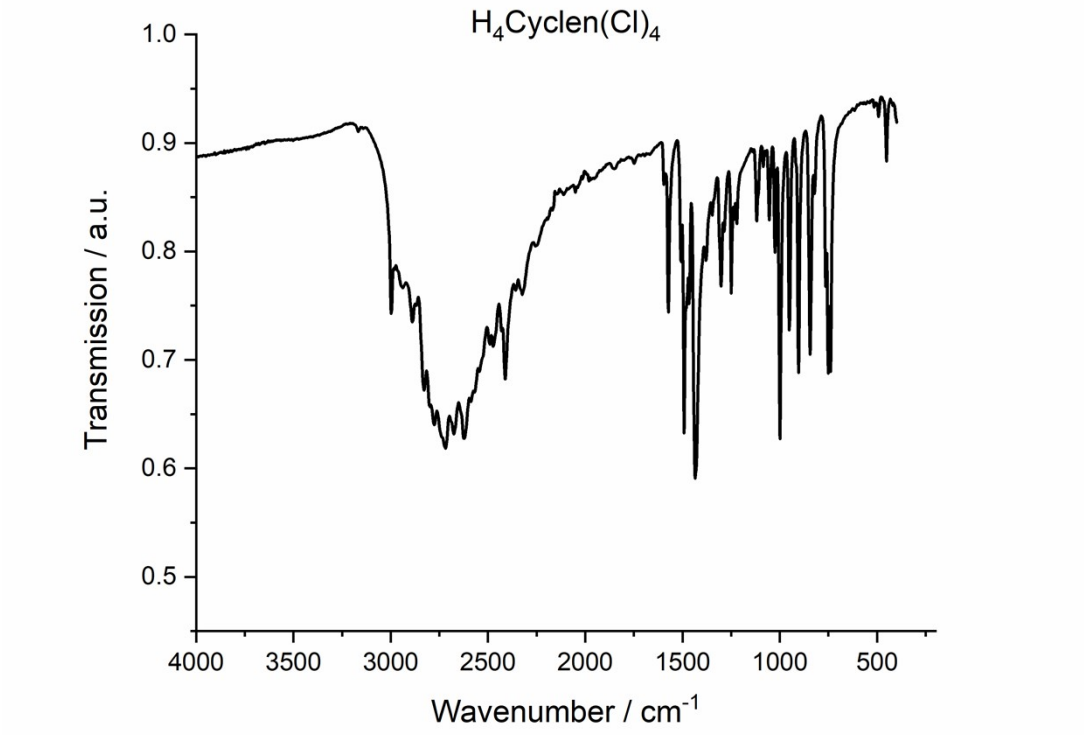

Figure S 6: FT-IR spectra of H_4cyclen(Cl)$_4$.

Characteristic IR bands (in cm^{-1}):

2997 (N-H stretching, amine salt/ C-H stretching, alkane); 2939 (N-H stretching, amine salt/ C-H stretching, alkane); 2889 (N-H stretching, amine salt/ C-H stretching, alkane); 2829 (N-H stretching, amine salt/ C-H stretching, alkane); 2800 (N-H stretching, amine salt/ C-H stretching, alkane); 2778 (secondary NH_2^+ overtone); 2719 (secondary NH_2^+ overtone); 2675 (secondary NH_2^+ overtone); 2622 (secondary NH_2^+ overtone); 2588 (secondary NH_2^+ overtone); 2569 (secondary NH_2^+ overtone); 2544 (secondary NH_2^+ overtone); 2492 (secondary NH_2^+ overtone); 2473 (secondary NH_2^+ overtone); 2429 (secondary NH_2^+ overtone); 2412 (secondary NH_2^+ overtone); 2358 (secondary NH_2^+ overtone); 2324 (secondary NH_2^+ overtone); 2257 (secondary NH_2^+ overtone); 1595 (N-H bending, amine); 1573 (N-H bending, amine); 1507 (-) ; 1492 (-); 1480 (-); 1466 (C-H bending, alkane); 1435 (-); 1379 (-); 1346 (-); 1302 (C-N stretching, aromatic amine); 1287 (-); 1250 (C-N stretching, amine) ; 1235 (-); 1221 (-); 1118 (C-N stretching, amine) ; 1085 (-); 1072 (-); 1054 (C-N stretching, amine); 1025 (-); 999 (-); 951 (-); 904 (-); 844 (-); 821 (-); 764 (-); 751 (-); 739 (-); 514 (-); 492 (-); 451 (-)

H_4Cyclen$(Br)_4$:

MW: 495.92 g/mol

Yield: 25.8 mg (0.0520 mmol, 18.6 %)

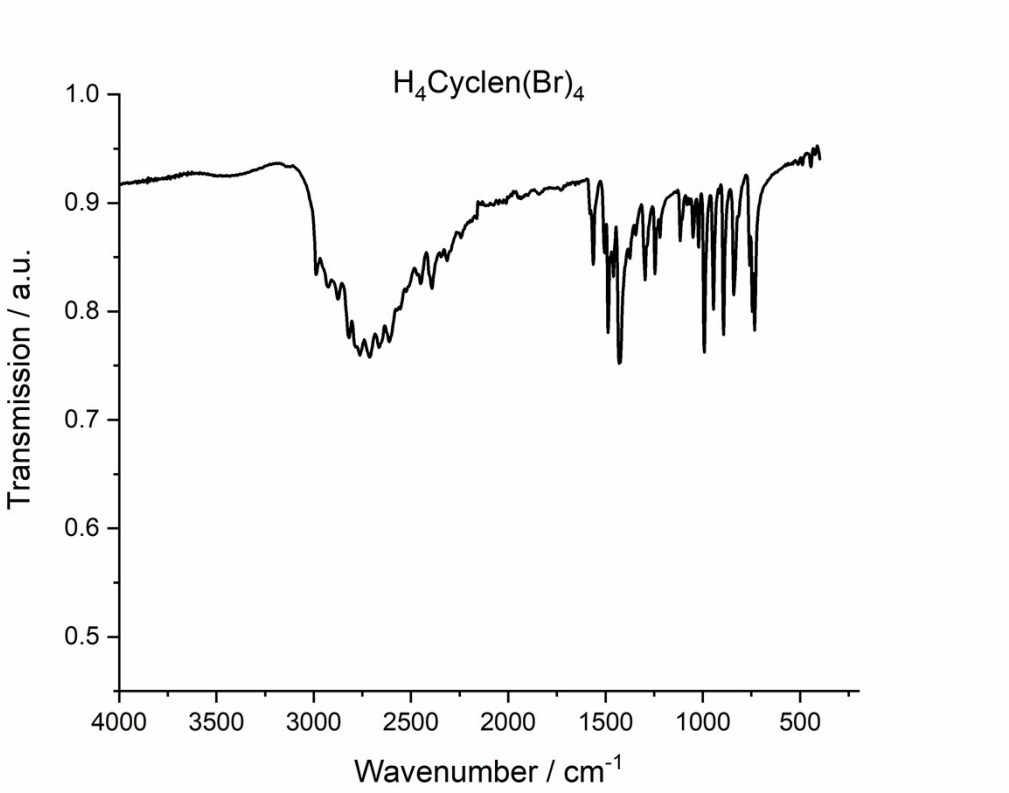

Figure S 7: FT-IR spectra of H_4cyclen$(Br)_4$

Characteristic IR bands (in cm^{-1}):

2987 (N-H stretching, amine salt/ C-H stretching, alkane); 2924 (N-H stretching, amine salt/ C-H stretching, alkane); 2874 (N-H stretching, amine salt/ C-H stretching, alkane); 2819 (N-H stretching, amine salt/ C-H stretching, alkane); 2785 (secondary NH_2^+ overtone); 2764 (secondary NH_2^+ overtone); 2711 (secondary NH_2^+ overtone); 2664 (secondary NH_2^+ overtone); 2612 (secondary NH_2^+ overtone); 2570 (secondary NH_2^+ overtone); 2555 (secondary NH_2^+ overtone); 2526 (secondary NH_2^+ overtone); 2469 (secondary NH_2^+ overtone); 2450 (secondary NH_2^+ overtone); 2393 (secondary NH_2^+ overtone); 2344 (secondary NH_2^+ overtone); 2314 (secondary NH_2^+ overtone); 2242 (secondary NH_2^+ overtone); 1580 (N-H bending, amine); 1563 (N-H bending, amine); 1506 (-); 1487 (-); 1474 (-); 1459 (C-H bending, alkane); 1431 (-); 1424 (-); 1375 (-); 1345 (-); 1297 (C-N stretching, aromatic amine); 1285 (-); 1245 (C-N stretching, amine); 1233 (-); 1221 (-); 1115 (C-N stretching, amine); 1106 (-); 1081 (-); 1067 (-); 1050 (C-N stretching, amine); 1022 (-); 992 (-); 945 (-); 893 (-); 840 (-); 816 (-); 759 (-); 745 (-); 733 (-); 510 (-); 488 (-); 444 (-); 423(-)

3. Crystallographic Information

Suitable single crystals were mounted onto a microloop using Fomblin oil. X-ray diffraction intensity data were measured at 150 K on a Bruker D8 QUEST diffractometer λ(MoKα = 0.71073 Å) equipped with a graphite monochromator. Structure solution was carried out using SHELX-2013[S6] package through OLEX2.[S7, S8] Corrections for incident and diffracted beam absorption effects were applied using empirical methods.[S9] Structures were solved by a combination of direct methods and difference Fourier syntheses and refined against F2 by the full matrix least-squares technique. Non-hydrogen atoms were refined anisotropically. Hydrogen atoms were added to carbon atoms using a riding model. The single crystals have twinning properties in the tetragonal space group and were correct by the Twin Law [010; 100;00-1] and by a basf parameter. The metal oxo framework was refined fully anisotropically. One solvent DMSO molecule was severely disordered, and restraints (ISOR, SIMU, DELU and SADI) were applied. The CIF files can be obtained free of charge from the CCDC.

Table S 2: Crystallographic parameters for the samples

	Compound (1)	**Compound (2):**	**Compound (3)**
CCDC number	2232429	2235427	2232423
Empirical formula	$La(DMSO)_8(C_8H_{22}N_4)[V_{12}O_{32}Br]$	$Ba(DMSO)_8(C_8H_{23}N_4)[V_{12}O_{32}Br]$	$La(DMSO)_8(C_8H_{22}N_4)[V_{12}O_{32}Cl]$
Formula weight	2455.94	2454.37	2411.49
Temperature/K	150.0	150.0	150.0
Crystal system	tetragonal	tetragonal	tetragonal
Space group	*P*4/n	P4/n	*P*4/n
a/Å	19.6945(5)	19.6360(13)	19.7197(10)
b/Å	19.6945(5)	19.6360(13)	19.7197(10)
c/Å	10.9545(4)	10.9821(11)	10.9727(6)
α/°	90	90	90.00
β/°	90	90	90.00
γ/°	90	90	90.00
Volume/Å³	4249.0(3)	4234.4(7)	4266.9(4)
Z	2	2	2
ρ_{calc}g/cm³	1.920	1.925	1.877
μ/mm⁻¹	2.595	2.568	2.147
F(000)	2456.0	2454.0	2420.0
Radiation	MoKα (λ = 0.71073)	MoKα (λ = 0.71073)	MoKα (λ = 0.71073)
2Θ range for data collection/°	3.718 to 54.224	3.708 to 55.166	3.72 to 54.14
Index ranges	$-25 \le h \le 25$, $-24 \le k \le 25$, $-14 \le l \le 14$	$-25 \le h \le 25$, $-25 \le k \le 25$, $-14 \le l \le 14$	$-25 \le h \le 25$, $-25 \le k \le 25$, $-14 \le l \le 14$
Reflections collected	71161	200109	57952
Independent reflections	4581 [R_{int} = 0.1089, R_{sigma} = 0.0521]	4895 [R_{int} = 0.0666, R_{sigma} = 0.0146]	4698 [R_{int} = 0.0922, R_{sigma} = 0.0368]
Data/restraints/parameters	4581/84/279	4895/42/279	4698/54/286
Goodness-of-fit on F²	1.048	1.115	1.079
Final R indexes [I>=2σ (I)]	R_1 = 0.0379, wR_2 = 0.0974	R_1 = 0.0258, wR_2 = 0.0634	R_1 = 0.0308, wR_2 = 0.0693
Final R indexes [all data]	R_1 = 0.0430, wR_2 = 0.1001	R_1 = 0.0343, wR_2 = 0.0698	R_1 = 0.0353, wR_2 = 0.0722
Largest diff. peak/hole / e Å⁻³	1.46/-0.79	1.04/-0.46	0.82/-0.48

4. Packing Diagram of compounds 1 – 8

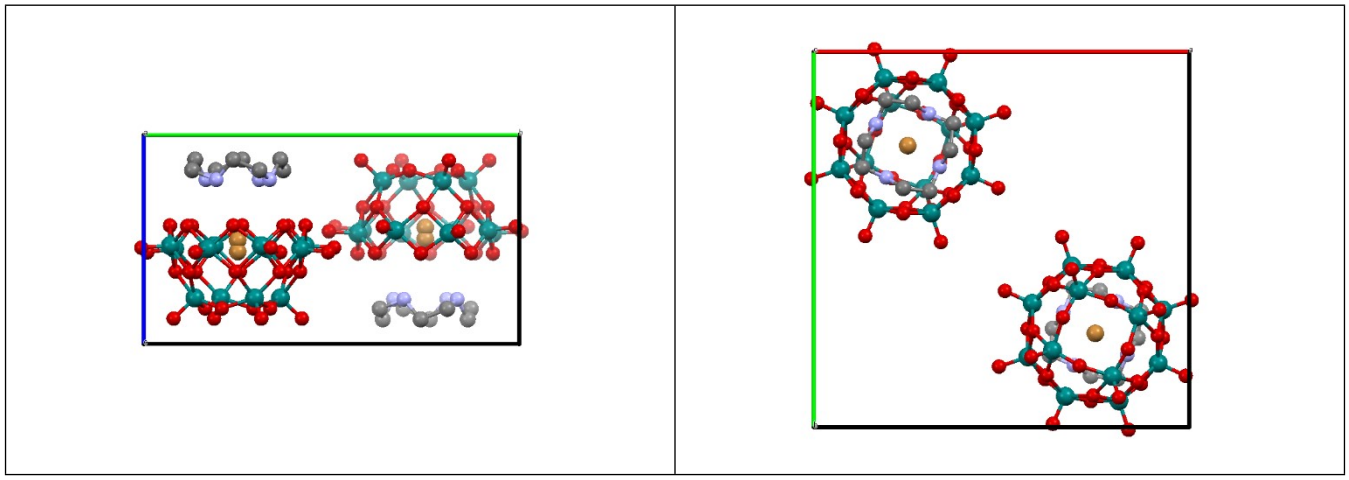

*Figure S 8: Packing diagram of compound **1** orientated along the a-axis(left) and c-axis(right) direction. The counteraction and DMSO solvent are omitted for clarity.*

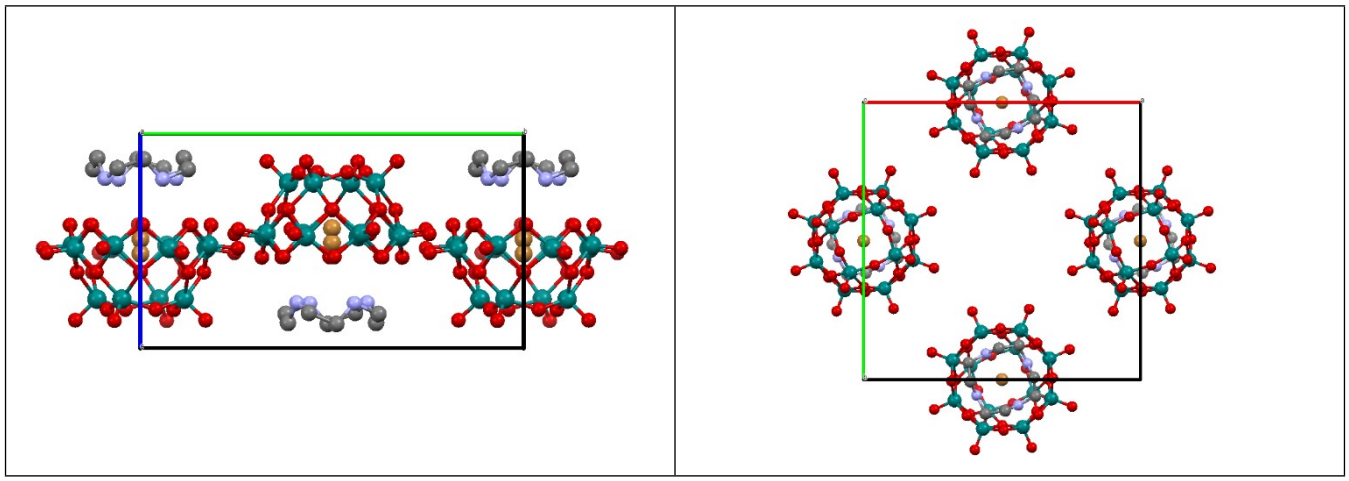

*Figure S 9: Packing diagram of compound **2** orientated along the a-axis(left) and c-axis(right) direction. The counteraction and DMSO solvent are omitted for clarity.*

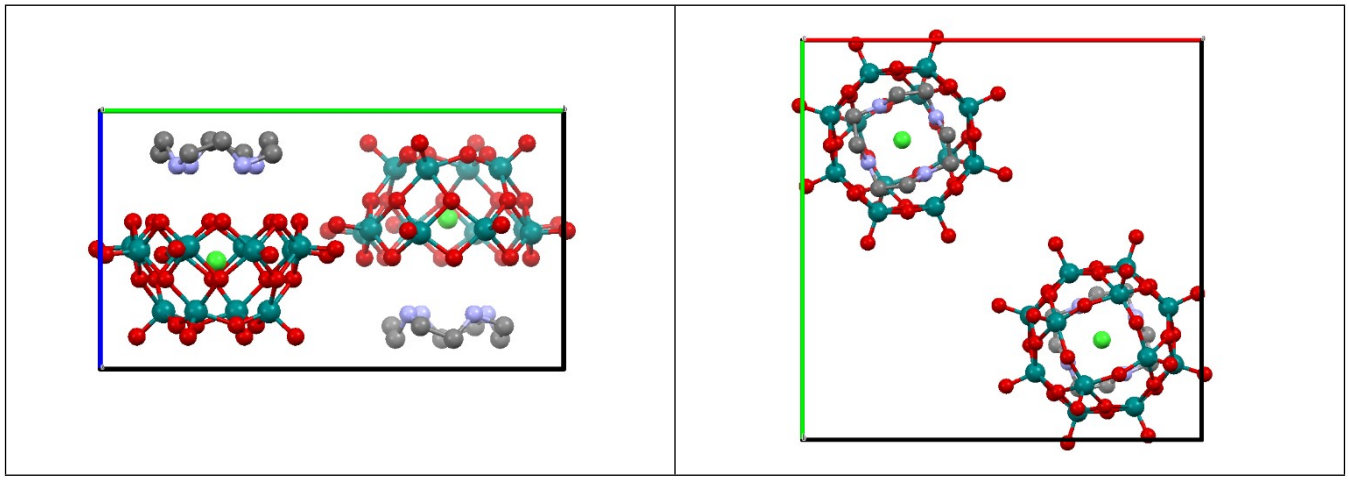

*Figure S 10: Packing diagram of compound **3** orientated along the a-axis(left) and c-axis(right) direction. The counteraction and DMSO solvent are omitted for clarity.*

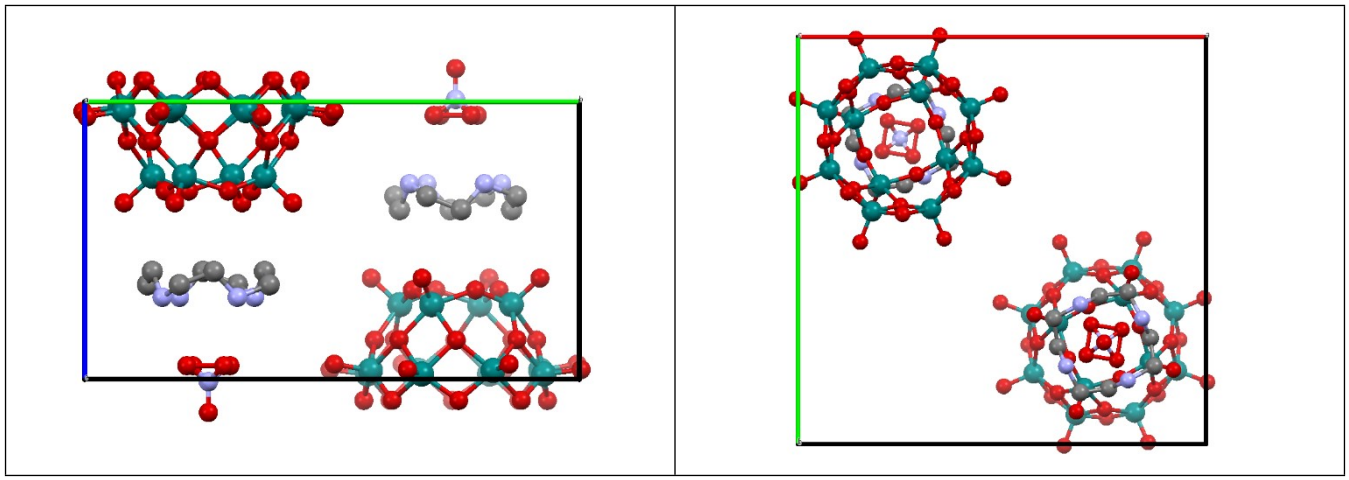

*Figure S 11: Packing diagram of compound **4** orientated along the a-axis(left) and c-axis(right) direction. The counteraction and DMSO solvent are omitted for clarity.*

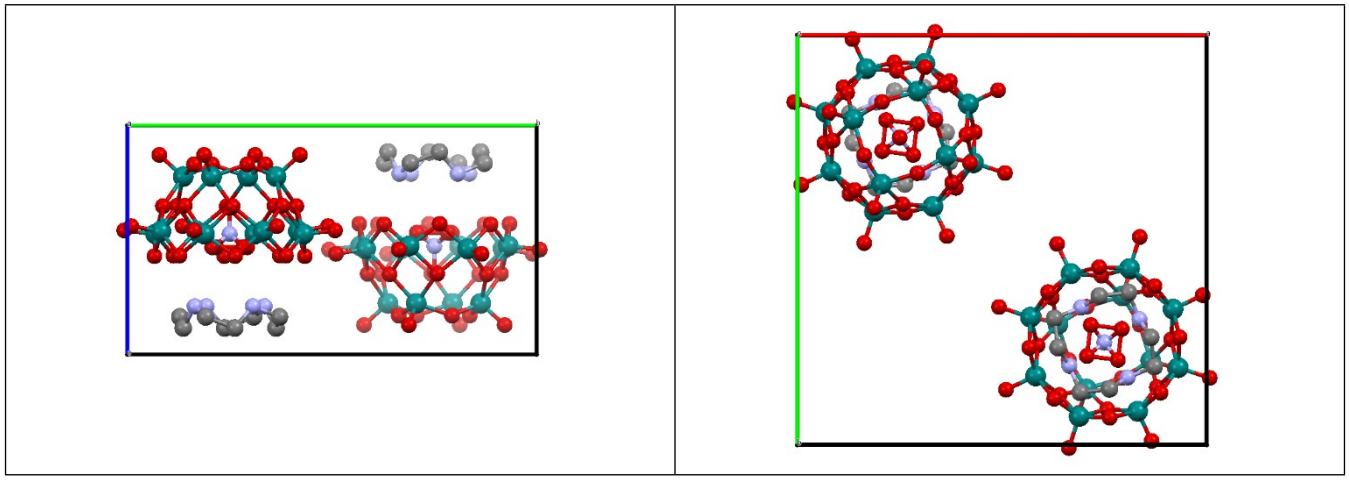

*Figure S 12: Packing diagram of compound **5** orientated along the a-axis(left) and c-axis(right) direction. The counteraction and DMSO solvent are omitted for clarity.*

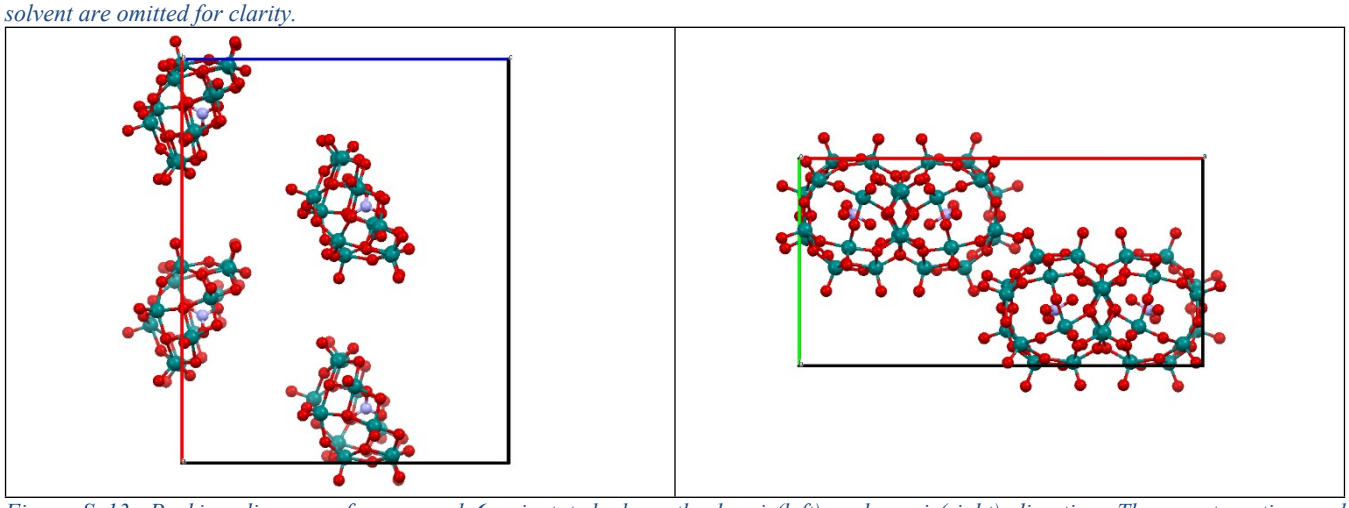

*Figure S 13: Packing diagram of compound **6** orientated along the b-axis(left) and c-axis(right) direction. The counteraction and Nitromethane solvent are omitted for clarity.*

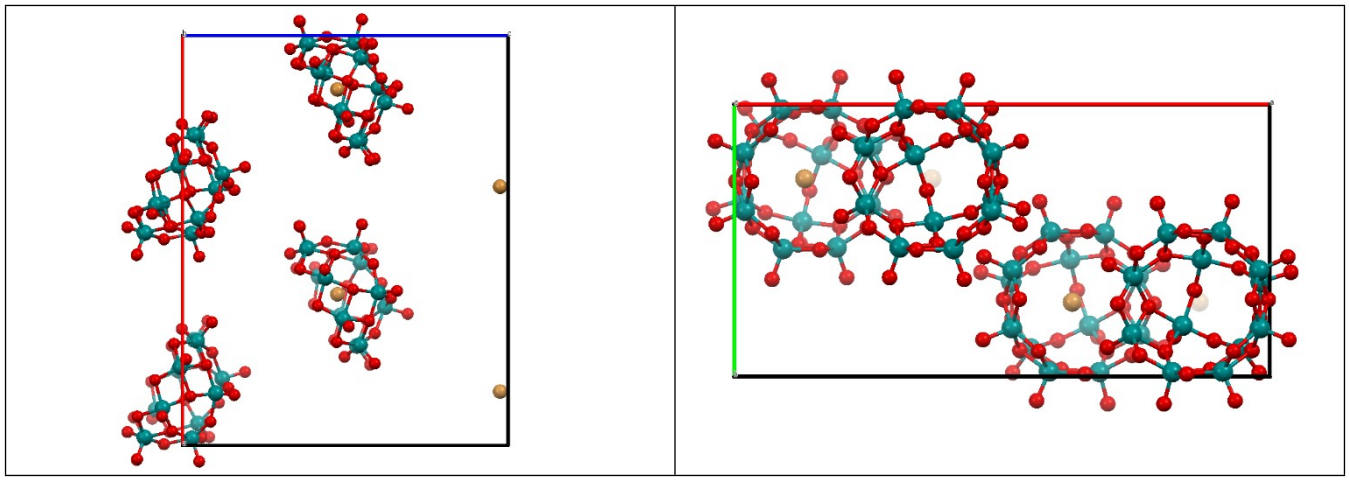

*Figure S 14: Packing diagram of compound **7** orientated along the b-axis(left) and c-axis(right) direction. The counteraction and Nitromethane solvent are omitted for clarity.*

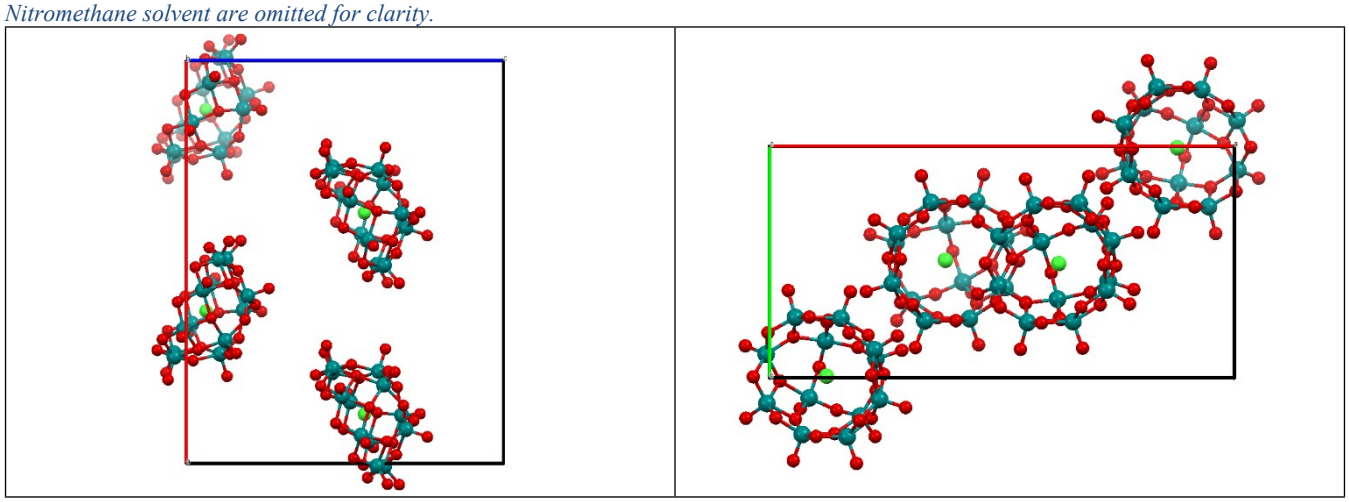

*Figure S 15: Packing diagram of compound **8** orientated along the b-axis(left) and c-axis(right) direction. The counteraction and Nitromethane solvent are omitted for clarity.*

5. Hirshfeld Surface Analysis

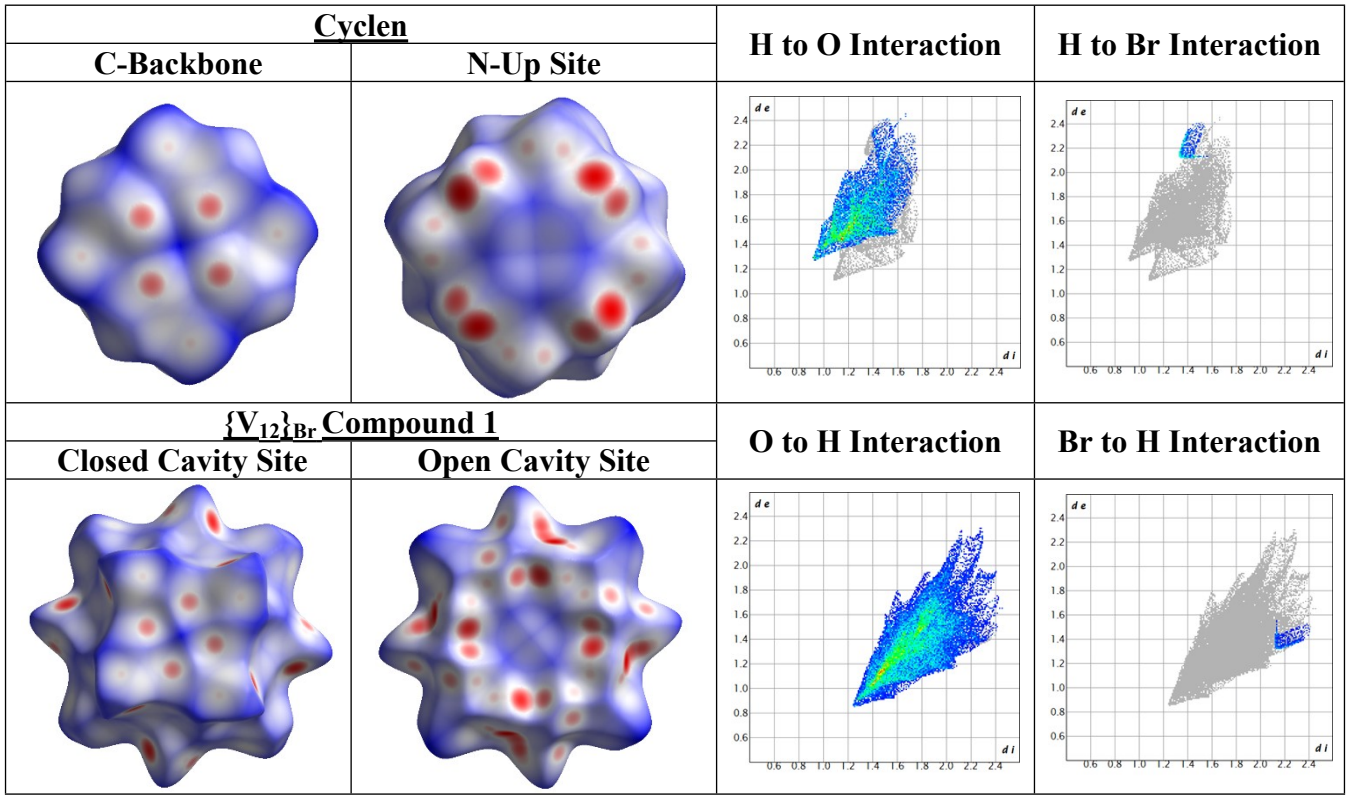

Figure S 16: Left: Hirshfeld surface analysis (surface plot: d_{norm}) of intermolecular interactions for cyclen (top) and ***{V12}Br*** *Compound* ***1*** *(bottom), highlighting the strong interactions at the hydrogen bonded interaction sites between both components. Right: Hirshfeld interaction analyses (fingerprint plots) to identify strong and weak intermolecular interactions between cyclen and* ***{V12}Br*** *Compound* ***1*** *(based on analysis of d_i vs d_e, i.e., internal and external atomic distances from the calculated Hirshfeld surface).*

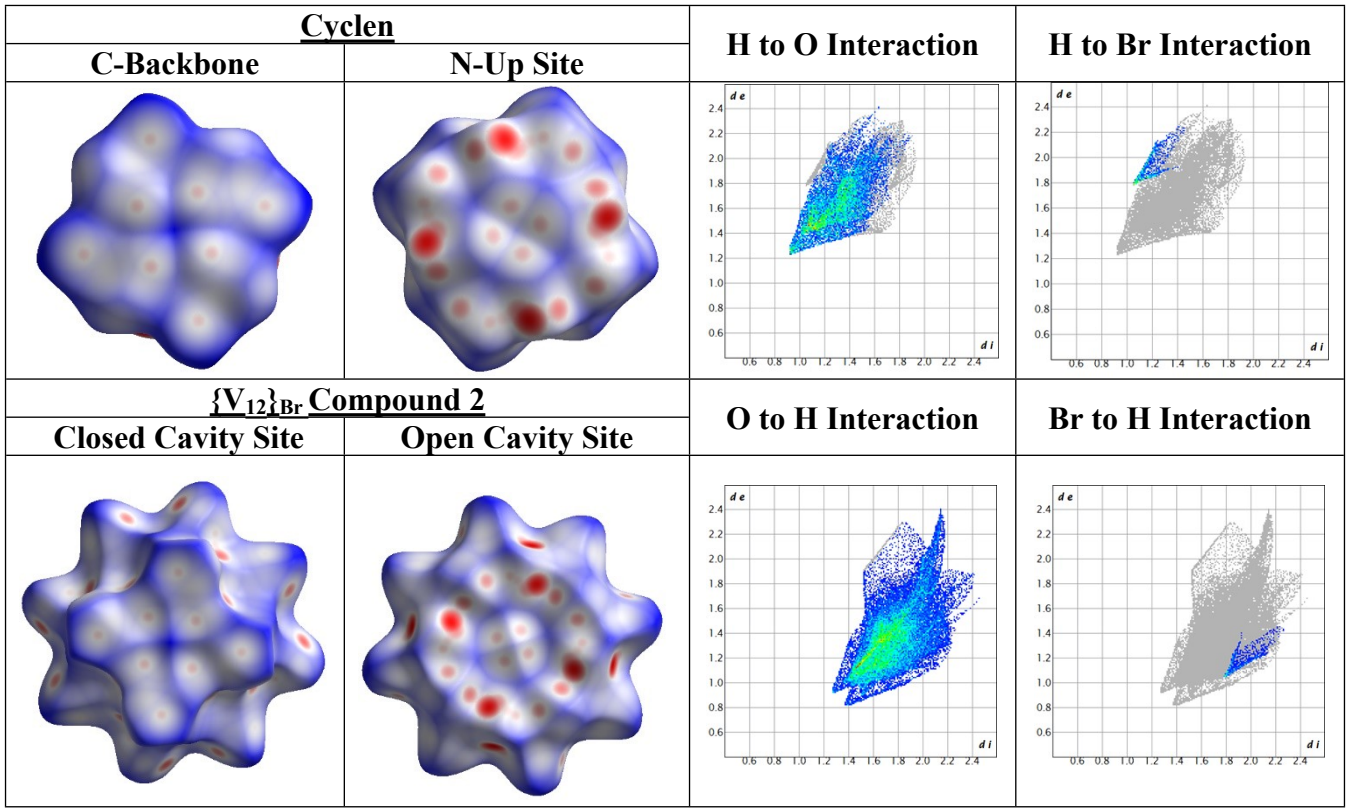

Figure S 17: Hirshfeld surface analysis (surface plot: d_{norm}) of intermolecular interactions for cyclen (top) and ***{V12}Br*** *Compound* ***2*** *(bottom), highlighting the strong interactions at the hydrogen bonded interaction sites between both components. Right: Hirshfeld interaction analyses (fingerprint plots) to identify strong and weak intermolecular interactions between cyclen and* ***{V12}Br*** *Compound* ***2*** *(based on analysis of d_i vs d_e, i.e., internal and external atomic distances from the calculated Hirshfeld surface).*

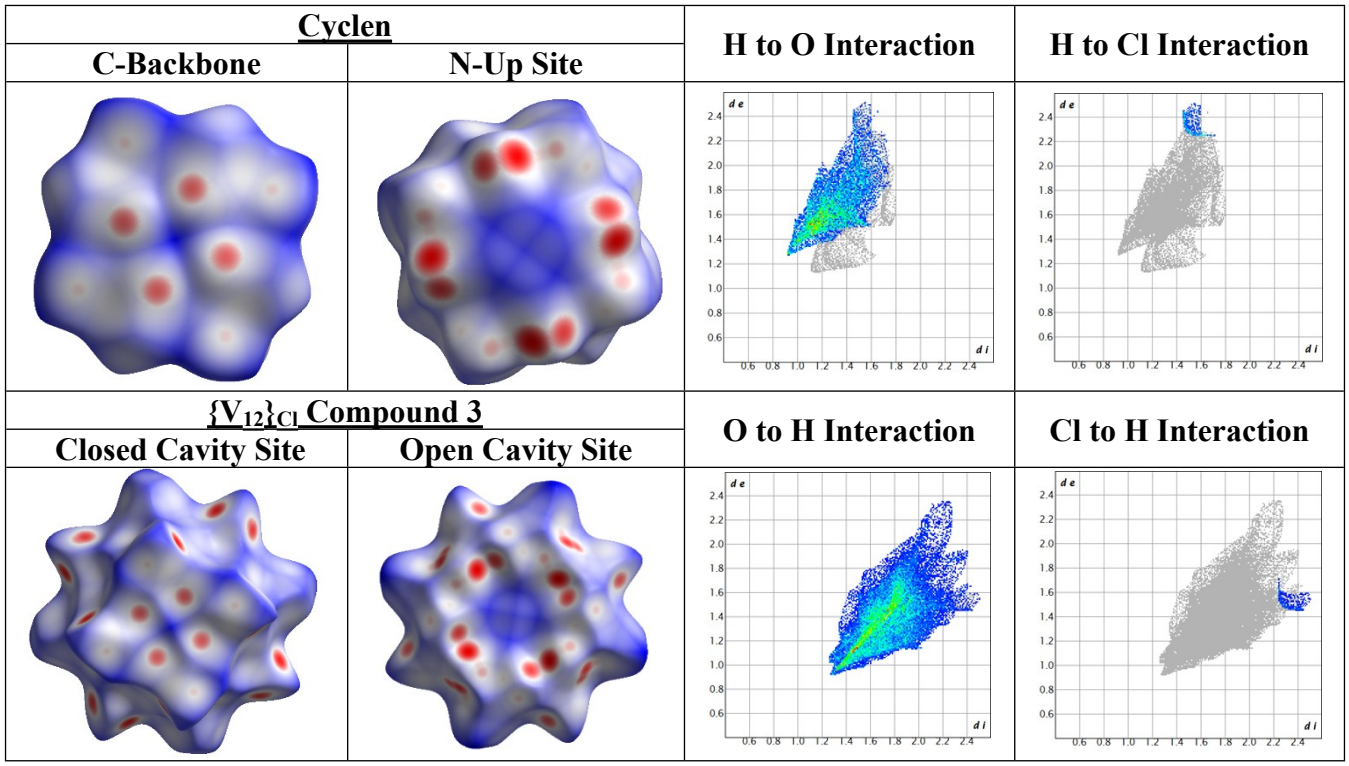

Figure S 18: Left: Hirshfeld surface analysis (surface plot: d_{norm}) of intermolecular interactions for cyclen (top) and ***{V12}Cl*** *Compound* ***3*** *(bottom), highlighting the strong interactions at the hydrogen bonded interaction sites between both components. Right: Hirshfeld interaction analyses (fingerprint plots) to identify strong and weak intermolecular interactions between cyclen and* ***{V12}Cl*** *Compound* ***3*** *(based on analysis of d_i vs d_e, i.e., internal and external atomic distances from the calculated Hirshfeld surface).*

6. TGA Studies

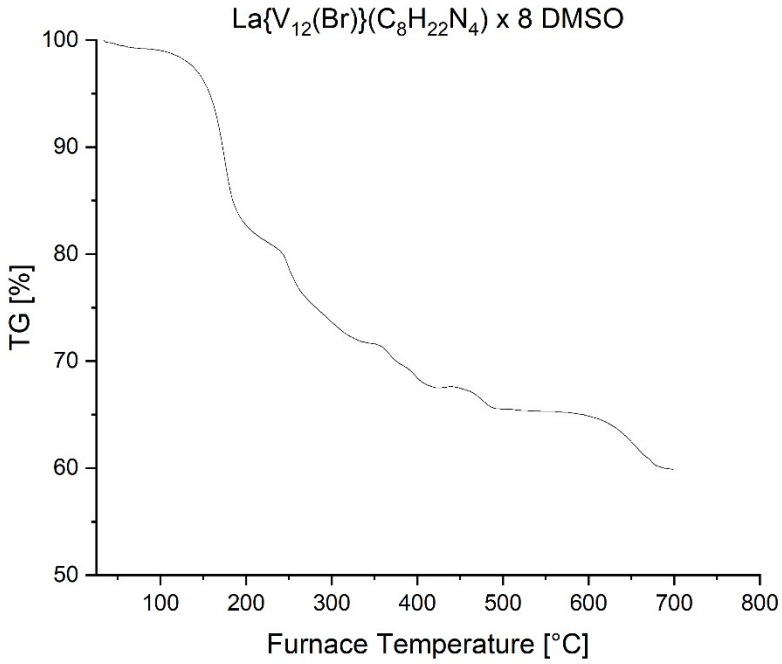

*Figure S 19: Thermogravimetric analysis (under air) of compound **1** the combined **{V_{12}}** with Cyclen and La as a counter cation and Bromide as a template. A weight loss of ca. 21.28 wt.-% between 25 °C and 240 °C is shown, which corresponds to diprotonated cyclen and three DMSO molecules (calc.: 20.22 wt.-%). Further weight loss of ca. 17.10 wt.-% between 240 °C and 500 °C, corresponds to the loss of five further DMSO molecules (calc.: 19.33 wt.-%).*

7. Infrared spectroscopy

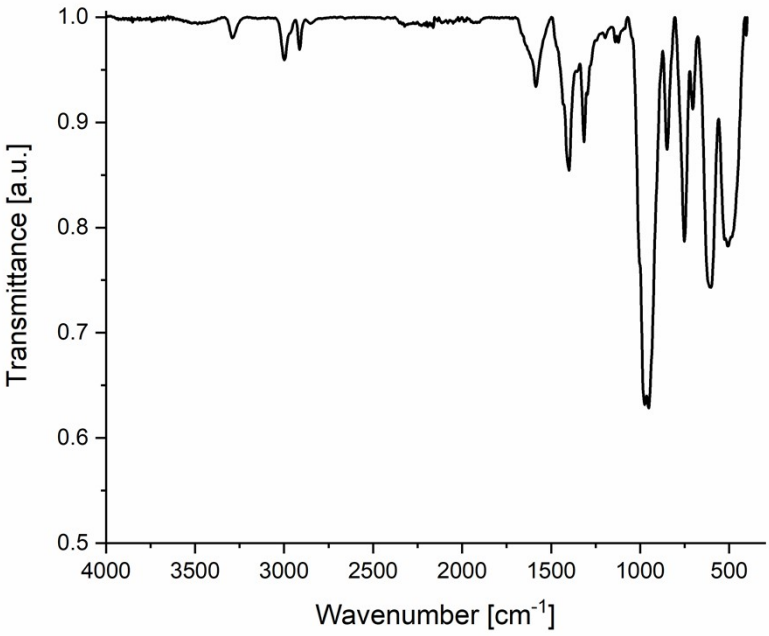

*Figure S 20: ATR-FT-IR spectra of compound **1**.*

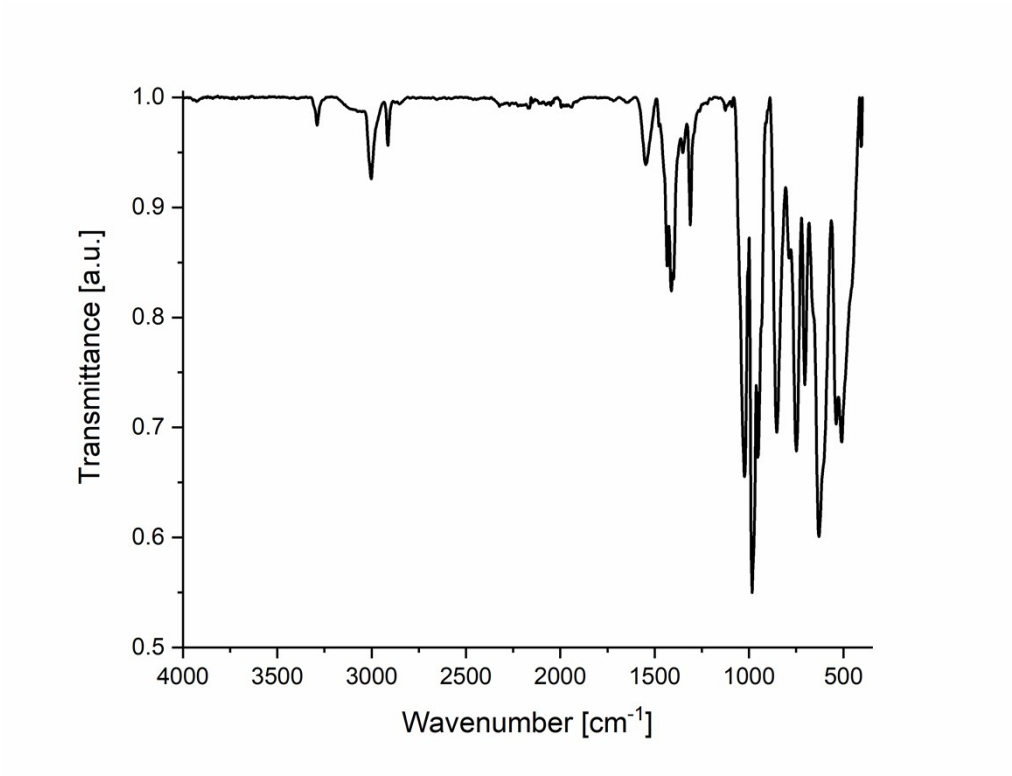

*Figure S 21: ATR-FT-IR spectra of compound **2**.*

8. ^{51}V-NMR in solution

^{51}V-NMR characterization and comparison to the literature

Table S 3: Summary of the observed ^{51}V NMR chemical shifts with and without Cyclen depending on the template.

Compound	^{51}V Chemical Shift Template: NO_3 [ppm]	^{51}V Chemical Shift Template: Br [ppm]
4 and 2	- 564, - 573, - 585, - 593, - 600, - 605	- 575, - 589, - 593, - 600, - 604
6 and 7	- 569, - 588, - 598, - 602	- 563, - 583, - 588, - 600

Acidification studies

The synthetic system reactivity with acid was probed as follows: 20.0 mg (0.0139 mmol) **{V_4}**, 2.40 mg cyclen (0.0139 mmol) and 2.40 mg (0.0092 mmol) $Ba(NO_3)_2$ were dissolved in 1 mL DMSO. 3 M aqueous HNO_3 was added in 10 ml aliquots, followed by recording ^{51}V NMR experiments. As shown below, addition of acid results in the loss of the precursor **{V_4}** signal and emergence of the characteristic **{V_{12}}$_{NO3}$** signals. Further acidification leads to cluster decomposition as observed by unassigned signals at – 478 ppm.

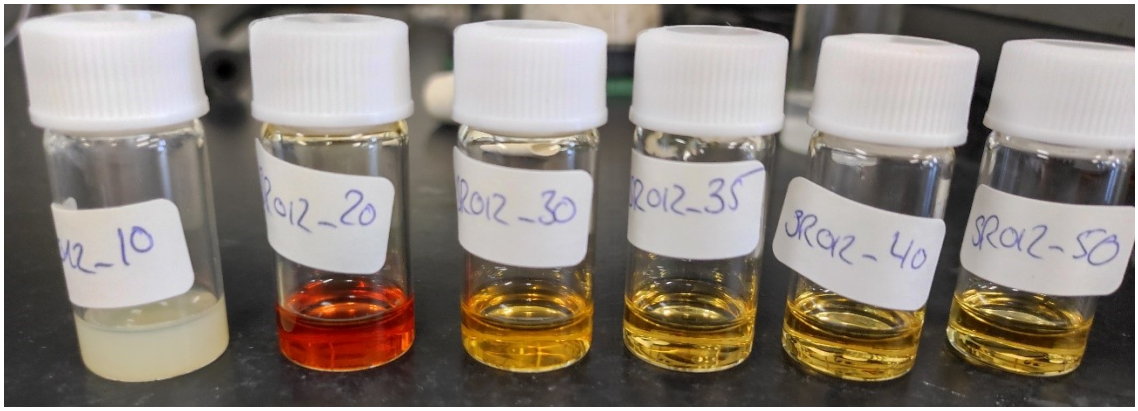

Figure S 22: Prepared solutions acidified by different amount of 3 M HNO_3.

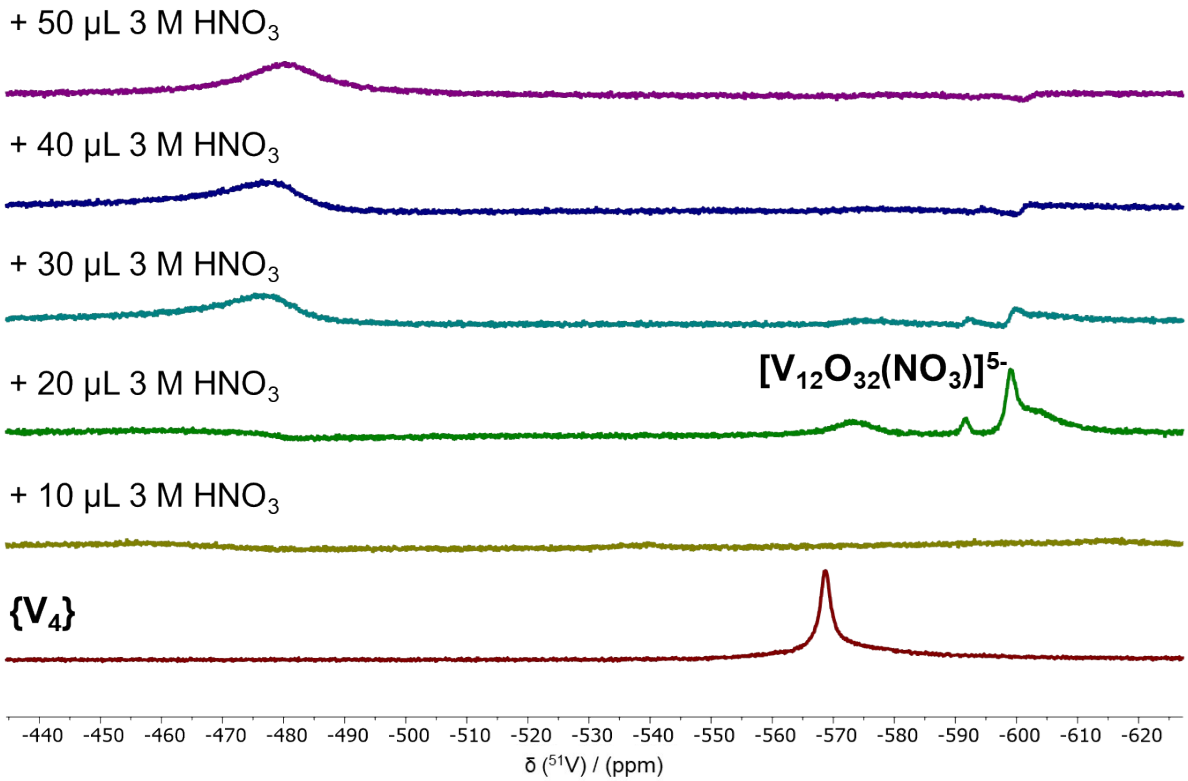

Figure S 23: ^{51}V NMR spectra throughout the acidification process.

Table S 4: Summary of the observed ^{51}V NMR signals by preparing the precursor solution and adding 3M HNO_3.

Sample	^{51}V NMR chemical shift [ppm]
Initial solution	-569
+ 10 µL 3M HNO_3	-No signal observed
+ 20 µL 3M HNO_3	- 573, - 591, - 599, - 604
+ 30 µL 3M HNO_3	- 477, - 592, - 600
+ 40 µL 3M HNO_3	- 478
+ 50 µL 3M HNO_3	- 480

Conversion of $\{V_4\}$ to $\{V_{12}\}$ with different templates

For the experiment 20.0 mg (0.0139 mmol) **$\{V_4\}$** were dissolved in 1 mL DMSO. To that solution, different amounts of the protonated $H_4cyclen(NO_3/Cl/Br)_4$ salt were added as proton and template source. The corresponding ^{51}V NMR spectra below are presented in a stacked form to follow the transformation.

*Table S 5: Summary of the ^{51}V NMR chemical shift in ppm after addition of $H_4cyclen(NO_3)_4$ to **$\{V_4\}$**.*

Substance	^{51}V NMR chemical shift [ppm]
$\{V_4\}$ in DMSO	- 569
+ 0.1 Eq. $H_4cyclen(NO_3)_4$	- 566; - 569
+ 0.25 Eq. $H_4cyclen(NO_3)_4$	- 539; - 564; - 568; - 614
+ 0.5 Eq. $H_4cyclen(NO_3)_4$	- 537; - 563; - 567; - 614
+ 1.0 Eq. $H_4cyclen(NO_3)_4$	- 574; -591; -599; -603

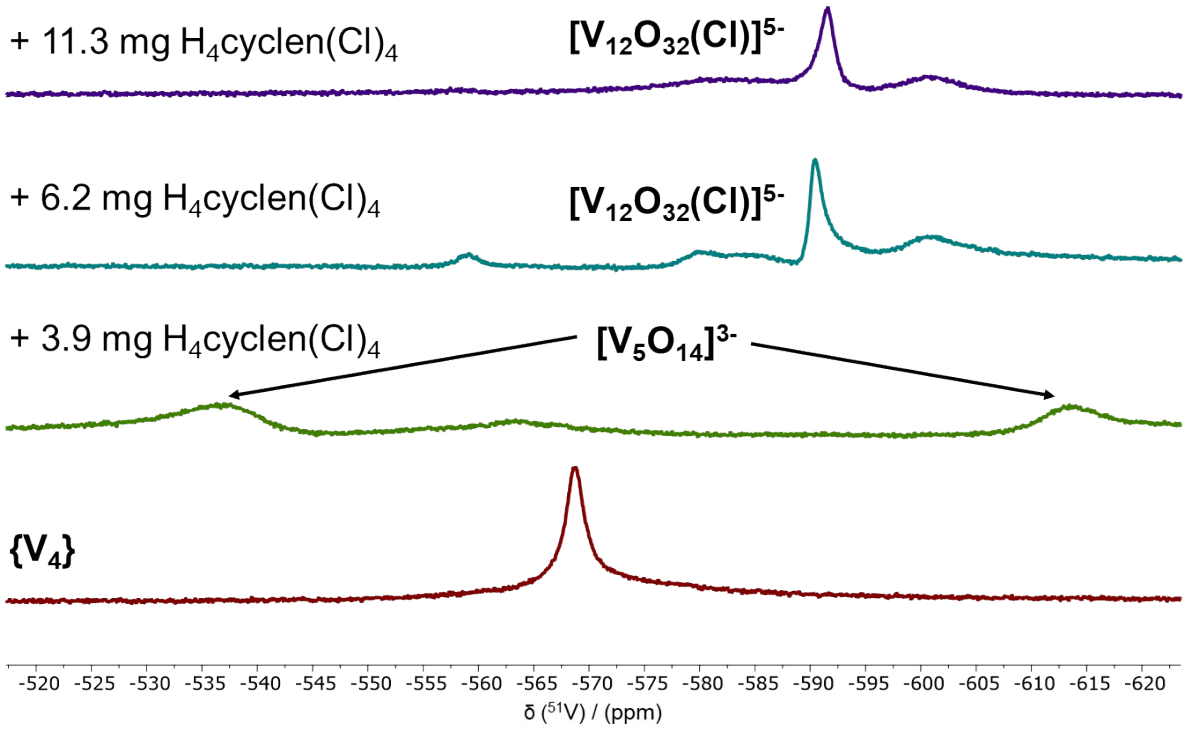

*Figure S 24: ^{51}V-NMR of **$\{V_4\}$** and after addition of different amount of $H_4cyclen(Cl)_4$ to the solution.*

*Table S 6: Summary of the NMR shift in ppm of adding $H_4cyclen(Cl)_4$ to **$\{V_4\}$**.*

Substance	^{51}V chemical shift NMR [ppm]
$\{V_4\}$ in DMSO	- 569
+ 3.9 mg $H_4cyclen(Cl)_4$	- 537; - 564; - 614
+ 6.2 mg $H_4cyclen(Cl)_4$	- 559; - 580; - 590; - 600
+ 11.3 mg $H_4cyclen(Cl)_4$	- 581; - 592; - 601

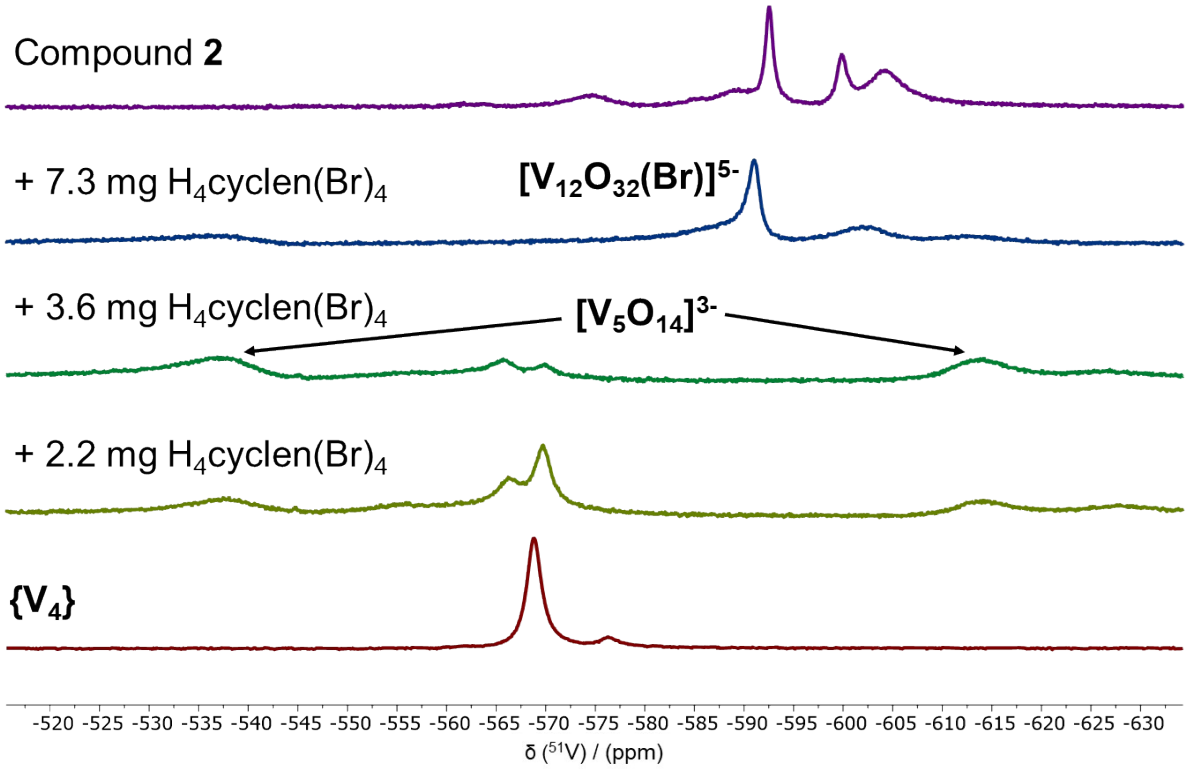

*Figure S 25: ^{51}V-NMR of **{V_4}** by adding different amount of H_4cyclen(Br)$_4$ to the solution.*

*Table S 7: Summary of the NMR shift in ppm of adding H_4cyclen(Br)$_4$ to **{V_4}**.*

Substance	^{51}VNMR chemical shift [ppm]
{V_4} in DMSO	- 569; - 576
+ 2.2 mg H_4cyclen(Br)$_4$	- 538; - 566; - 570; -615
+ 3.6 mg H_4cyclen(Br)$_4$	- 538; - 566; - 570; - 614
+ 7.3 mg H_4cyclen(Br)$_4$	- 536; - 591; - 602
Compound 2	- 575, -590, -593, -600, -604

Synthesis of $\{V_{12}(X)\}$ in the Presence of Cyclen

Solutions of $(n\text{Bu}_4\text{N})_5\{V_{12}O_{32}(NO_3)\}$ or $(n\text{Bu}_4\text{N})_5\{V_{12}O_{32}(\text{Br})\}$ (0.015 mmol) were prepared in DMF/propylene carbonate (1 ml, 1:1, v:v). 1 eq. cyclen was added to the solution, and the solution was characterized by ^{51}V-NMR spectroscopy before and after cyclen addition.

Table S 8: Summary of ^{51}V-NMR peak shifts of $TBA_5\{V_{12}O_{32}(NO_3)\}$ and $TBA_5\{V_{12}O_{32}(Br)\}$ in absence and presence of cyclen.

Substance	^{51}V chemical shift NMR [ppm]
$(n\text{Bu}_4\text{N})_5\{V_{12}O_{32}(NO_3)\}$	- 567, - 580, - 588, - 595, - 598, - 602
$(n\text{Bu}_4\text{N})_5\{V_{12}O_{32}(NO_3)\}$+ Cyclen	- 538, - 565, - 576, - 590, - 602, - 606, - 613
$(n\text{Bu}_4\text{N})_5\{V_{12}O_{32}(\text{Br})\}$	- 563, - 584, - 588, - 600
$(n\text{Bu}_4\text{N})_5\{V_{12}O_{32}(\text{Br})\}$ + Cyclen	- 562, - 569, - 572, - 587, -591, - 603

9. Solid State NMR spectroscopy

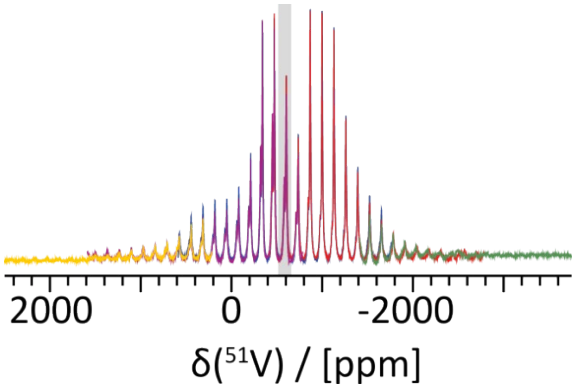

Figure S 26: ^{1}H-^{51}V cross-polarization (CP) NMR data were measured with a contact time of 2 ms at 13.8 kHz. Additional variable offset NMR spectra (yellow, purple, red, blue, green) were recorded to yield a full spectral pattern for this compound.

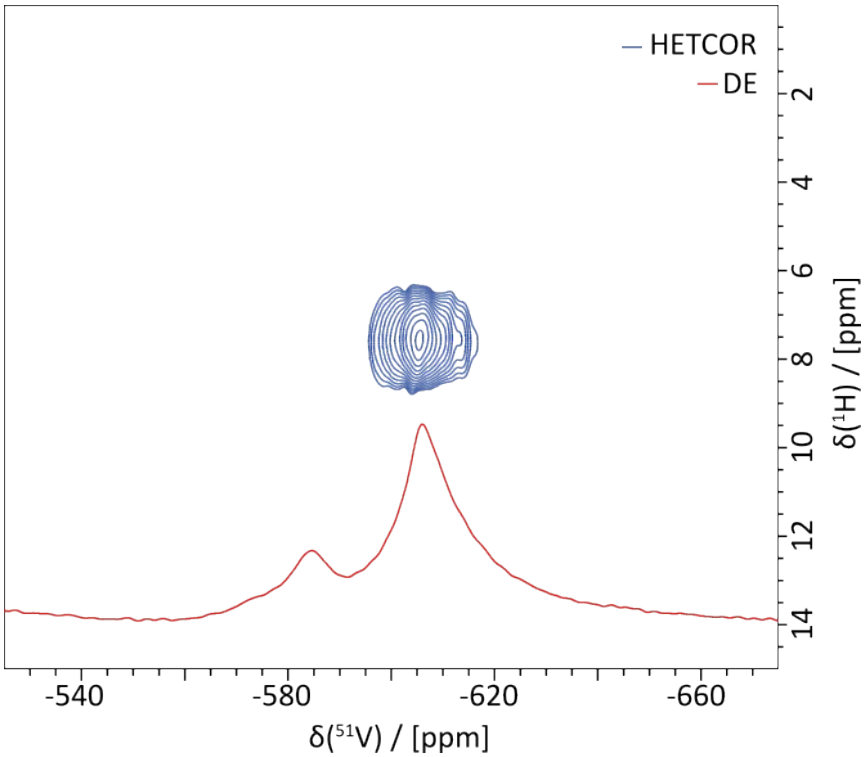

*Figure S 27: ^{1}H-^{51}V FSLG HETCOR spectrum of **$Ba\{V_{12}\}_{NO3}$**.*

10. Reference:

S1: Spackman, P. R. *et al. CrystalExplorer* : a program for Hirshfeld surface analysis, visualization and quantitative analysis of molecular crystals. *J. Appl. Crystallogr.* **54**, 1006–1011 (2021).

S2: Forster, J., Rösner, B., Khusniyarov, M. M. & Streb, C. Tuning the light absorption of a molecular vanadium oxide system for enhanced photooxidation performance. *Chemical Communications* **47**, 3114 (2011).

S3: Kuwajima, S., Kikukawa, Y. & Hayashi, Y. Small-Molecule Anion Recognition by a Shape-Responsive Bowl-Type Dodecavanadate. *Chem Asian J* **12**, 1909–1914 (2017).

S4: Kuwajima, S. *et al.* A Bowl-Type Dodecavanadate as a Halide Receptor. *ACS Omega* **2**, 268–275 (2017).

S5: Warden, A. C., Warren, M., Hearn, M. T. W. & Spiccia, L. Anion binding to azamacrocycles: Synthesis and X-ray crystal structures of halide adducts of [12]aneN4 and [18]aneN6. *New Journal of Chemistry* **28**, 1160–1167 (2004).

S6: Bourhis, L. J., Dolomanov, O. v., Gildea, R. J., Howard, J. A. K. & Puschmann, H. The anatomy of a comprehensive constrained, restrained refinement program for the modern computing environment – *Olex2* dissected. *Acta Crystallogr A* **71**, 59–75 (2015).

S7: Dolomanov, O. v., Bourhis, L. J., Gildea, R. J., Howard, J. A. K. & Puschmann, H. *OLEX2* : a complete structure solution, refinement and analysis program. *J Appl Crystallogr* **42**, 339–341 (2009).

S8: Sheldrick, G. M. A short history of *SHELX*. *Acta Crystallogr A* **64**, 112–122 (2008).

S9: Blessing, R. H. An empirical correction for absorption anisotropy. *Acta Crystallogr A* **51**, 33–38 (1995).